# Combined impact of selected material properties and environmental conditions on the swelling pressure of compacted claystone/bentonite mixtures

Marvin Middelhoff, O. Cuisinier, F. Masrouri, J. Talandier, N. Conil

# Combined impact of selected material properties and environmental conditions on the swelling pressure of compacted claystone/ bentonite mixtures

M. Middelhoff [1, 2]*, O. Cuisinier [1], F. Masrouri [1], J. Talandier [2], N. Conil [2]

[1] Université de Lorraine – LEMTA, UMR 7563 CNRS,
(2 Rue du Doyen Marcel Roubault - BP 10162, 54505 Vandœuvre-lès-Nancy CEDEX, France)

[2] Agence nationale pour la gestion des déchets radioactifs (ANDRA), France

Marvin.Middelhoff@univ-lorraine.fr

Abstract: Mixtures composed of 70% crushed Callovo-Oxfordian claystone and 30% MX80-bentonite are considered as materials, that could be used for backfilling a future radioactive waste repository in deep sedimentary rock formations. Their characterization is of interest, as the replacement of fractions of crushed claystone by bentonite enhances the chemo-hydro-mechanical performance of backfill. The materials are envisaged to be installed directly in the drifts and shafts by means of conventional compaction techniques. The hydro-mechanical behavior of materials containing expansive mineral phases, and especially their swelling behavior, is known to be significantly affected by the initial material properties and environmental and stress conditions. The present study aimed to assess the combined impact of variations in the material properties and environmental conditions, particularly the grain size distribution, dry density and saturating solution chemistry, on the swelling pressure of the mixtures, by conducting a comprehensive laboratory experimental program. The results revealed that the adjustment of the grain size distribution of employed bentonite enhanced the compaction behavior and, in turn, the swelling behavior of the mixtures. Generally, swelling pressures of mixtures were less affected by the employed saline and alkaline solutions than those of crushed claystone. The measured swelling pressures were exponentially related to the initial dry density of the expansive mineral phase, regardless of the grain size distribution. Based upon the finding that the expansive mineral phase being present in crushed claystone contributed to measured swelling pressures, a new approach was introduced to calculate the dry density of the expansive mineral phase in bentonites and their mixtures with non-expansive or less-expansive materials.

Keywords: Callovo-Oxfordian claystone, MX80-bentonite, Swelling pressure, Grain-size distribution, Dry density, Solution chemistry

Highlights:

- Grain size distribution of bentonite influenced material performance of the mixtures
- Adjusting the grain size distribution of bentonite increased the highest swelling pressure
- Solution chemistry had little impact on the short-term evolution of the swelling pressure
- Impact of expansive minerals in claystone on the swelling pressure was considered

# 1 Introduction

The long-term integrity of geological repository systems for nuclear waste is envisaged to be ensured by means of installing a multiple barrier system, which is generally composed of waste canisters, backfill, seals and the surrounding geological formation. The major containment might be either the geological formation or the canister, depending on the disposal concept.

According to Andra (2005), the French concept favors the former. It plans to install the future repository for disposing intermediate and high-level waste (ILW/ HLW) in the clay-rich Callovo-Oxfordian (COX) sedimentary rock formation, henceforth referred to as COX-claystone. Since the construction of drifts and shafts reduces the integrity of the geological formation, backfill and seals serve the general purpose of recovering the integrity upon terminating the closure-phase. Both are envisaged to fill hydraulic conductive voids and to limit the propagation of the excavation-damaged zone (EDZ) by stabilizing the surrounding rock mass. In addition, seals compress the EDZ, and fluxes of fluid phases from the repository to the biosphere and vice versa are inhibited by these means. Based on the mentioned purposes, the potential seal and backfill materials must exhibit a swelling potential, as well as strength. Specifically, the seal material must possess hydraulic conductivity, which ensures the inhibition of fluid fluxes. Andra (2005) proposed the employment of bentonite as a pure material or as a dominant fraction of a mixture with non- or less-expansive material, such as sand or crushed COX-claystone ($COX_c$), to seal the drifts and shafts. Conversely, backfill material consists of $COX_c$, which can be alternatively mixed with minor fractions of bentonite. The re-employment pursues the objectives of reducing the negative impact of backfill on the surrounding geological formation, avoiding mineralogical and physico-chemical incompatibilities, and lowering the costs by replacing commercial bentonite with $COX_c$. Determined in a manifold fashion, the hydro-mechanical behavior of materials containing expansive mineral phases is significantly

affected by the material properties, the stress history and the environmental conditions (Chen, 1988; Gens and Alonso, 1992).

Different techniques have been considered to install backfill and seals. Seals are constructed by emplacing either industrially fabricated blocks or pellets into the drifts and shafts. Their industrial fabrication offside is advantageous, since the initial dry density can be adapted to the target values by using, for instance, the required compaction energy. Conversely, the employment of conventional techniques, such as vibrating plates, is envisaged to compact backfill layer wise in situ. As the applicable compaction energy is limited in the case of in situ compaction, the initial dry density varies as a function of the initial water content. Generally, the maximum dry density is attained at the optimum water content by using constant compaction energy. The backfill is characterized by a lower initial dry density and a significantly higher water content, compared to blocks and pellets (Andra, 2005).

The feasibility of in situ compaction as a potential technique for backfill installation was evaluated by Gunnarson et al. (2001) and Johannesson (2014). They aimed to compact the backfill to the maximum dry density at the optimum water content, since the highest swelling pressure and low hydraulic conductivity are likely to be attained by this means (Mitchell and Soga, 2005). It was hardly realizable to homogeneously compact the material in the cross-section of the drift, especially close to the drift top and walls. They referred to the issues of the position of the compactor, which caused a loss of compaction energy and, in turn, a reduction in the initial dry density up to 20% with respect to the maximum dry density. Great differences in the swelling pressures were thus attributed to variations in these material properties.

In addition to varying material properties, evolving environmental conditions, such as saturating solution chemistry, are likely to have a negative impact on the performance of backfill materials containing expansive mineral phases. The phenomenon known as alkaline plume triggers the dissolution and modification of clay minerals in the backfill material, altering its

84 structure and, in turn, its performance (Bradbury and Baeyens, 2003; Pusch et al., 2003;
85 Karnland et al., 2007; Cuisinier et al., 2009; Cuisinier et al., 2014) These combined variations
86 in the material properties and environmental conditions can impair the performance of backfill
87 materials in such a way that formulated safety requirements are not met.

88 As information about $COX_c$ was limited, most studies performed within the last few years
89 were focused on characterizing the volume change and hydraulic conductivity behavior, rather
90 than considering additional variations in material properties and environmental conditions.

91 Tang et al. (2010), Tang et al. (2011a) and Tang et al. (2011b) compacted $COX_c$ to initial
92 dry densities of ≈ 2 $Mg/m^3$ at water contents of ≈ 3 %. These densities were in accordance with
93 the envisaged densities of blocks being employed for seal construction. The obtained results
94 indicated that the swelling pressures ranged from several hundreds of kPa to some MPa. The
95 measured hydraulic conductivities were equal to those of intact drill cores of COX. Wang et al.
96 (2012) and Wang et al. (2014) performed swelling pressure and free swell experiments on com-
97 pacted MX80-bentonite/ $COX_c$-mixtures, which were predominantly composed of MX80-ben-
98 tonite (≈ 70%). Their experiments considered not only a variety of soil properties and environ-
99 mental conditions but also time effects. Just like in the sand-bentonite mixtures, the magnitude
100 of material swelling was exponentially related to the initial dry density and was hardly affected
101 by the saturation with a solution of low ionic strength. It can be concluded that few studies have
102 examined mixtures of materials that each contains expansive mineral phases. Moreover, the
103 performed experimental programs have hardly considered the variations in the initial material
104 properties, as well as environmental conditions and their impact on the hydro-mechanical be-
105 havior of these mixtures.

106 This experimental program assessed the impact of replacing 30% of $COX_c$ with MX80-
107 bentonite on the structure, as well as the impacts on the compaction characteristics and on the
108 swelling pressure. In particular, the consideration of the total amount of expansive mineral

109 phases in these mixtures was of major interest, as the expansive mineral phases in $COX_c$ were
110 expected to contribute to the evolution of the swelling pressure. Bentonite was processed to
111 maximum grain sizes of 0.25 mm and 2.00 mm before being mixed with $COX_c$. Henceforth,
112 the mixtures of $COX_c$ with bentonite with maximum grain sizes of 0.25 mm and 2.00 mm are
113 referred to as the powder mixture and the grain mixture, respectively. The short-term develop-
114 ment of the swelling pressure was tested by adopting the constant-volume method. Based on
115 the findings of Gunnarson et al. (2001), the impact of varying the dry densities on the short-
116 term evolution of the swelling pressure was investigated by compacting the mixtures to their
117 maximum and reduced dry densities at the optimum water content. The complementing exper-
118 iments aimed to assess the impact of solutions with different pH values and ionic strengths on
119 samples that were compacted to their maximum dry density at the optimum water content.
120 Eventually, their combined impact on the performance of claystone/ bentonite-mixtures was
121 analyzed in terms of the swelling pressure.

122 ## 2 Theoretical Background

123 The impact of variations in the saturating solution chemistry and dry density on the swell-
124 ing behavior of claystone/ bentonite-mixtures is predominantly related to the physico-chemical
125 forces at the molecular scale, namely, attractive and repulsive forces, that occur when saturating
126 expansive clay minerals. These forces, in turn, are affected by the structure of the mixtures
127 (Mitchell and Soga, 2005).

128 The mineralogical composition of MX80-bentonite is dominated by montmorillonite
129 (Müller-Vonmoos and Kahr, 1983; Herbert et al., 2004; Karnland et al., 2007). Table 1 com-
130 piles information about the mineralogical composition of MX80-bentonite taken from the liter-
131 ature. Single montmorillonite particles are characterized by both their platy form and their var-
132 iable thickness. Their unit layers are composed of one alumina sheet that is sandwiched between
133 two silica sheets. The permanently negative surface charge at their basal planes is attributable

134 to isomorphous substitution, which is usually compensated by exchangeable cations, while the
135 surface charges at their edge faces vary as a function of the proton concentration in the solution.
136 Positively charged species are thus attracted by basal planes and either attracted or repelled by
137 the edge faces (van Olphen, 1977; Tombácz and Szekeres, 2004, 2006). Regardless of the sur-
138 face charge, dissolution and modification processes alter the clay minerals and their structures,
139 in cases where they are exposed to solutions of different pH (Bradbury and Baeyens, 2003).
140 These processes account for the sensitivity of expansive clays to varying pH values.

141 Apart from the pH, the swelling behavior of expansive clays is also affected by the ionic
142 strength of the solution. Once montmorillonite particles are saturated with aqueous solution,
143 the cations and water molecules are adsorbed by attractive forces on particle surfaces, forming
144 diffuse double layers. Water molecules additionally permeate the interlayer space due to the
145 higher hydration potential (Yong, 1999; Pusch and Yong, 2003). The concentration of the cat-
146 ions is high close to the particle surface and declines exponentially, as the distance from the
147 particle surface increases. Repulsive forces occur once the diffuse double layers of the neigh-
148 boring particles overlap (Bolt, 1956; Sridharan et al., 1986; Mitchell and Soga, 2005). Among
149 other factors, the thickness of the diffuse double layers varies as a function of the ion concen-
150 tration and ionic strength (Mitchell and Soga, 2005).

151 Swelling itself is comprised of two processes, namely, crystalline and osmotic swelling,
152 occurring upon hydration of expansive clay particles (Madsen and Müller-Vonmoos, 1989).
153 Among other factors, such as the interlayer cation nature, their magnitude is related to the pH
154 and ionic strength of the solution. Crystalline swelling is the result of the progressive hydration
155 of exchangeable cations in the interlayer space, while osmotic swelling is caused by the inter-
156 action of overlapping diffuse double layers formed on neighboring clay particles. More detailed
157 information about clay swelling is given in Madsen and Müller-Vonmoos (1989), Sridharan
158 and Choudhury (2002) and Schanz and Tripathy (2009). Swelling pressure can be considered

159 as the sum of hydration and repulsion forces, that accumulate upon saturation of expansive
160 clays under confined conditions. Conversely, free swell strains develop under free conditions
161 (Madsen and Müller-Vonmoos, 1989).

162 Attractive and repulsive forces account for the structure of the compacted expansive clays
163 at the micro- and macro-scales. However, their structure is hardly affected by the ionic strength
164 and pH of the adjacent solution. Generally, multiple clay particles form aggregates at the micro-
165 scale, in which the single particles are orientated predominantly parallel due to the repulsion of
166 equally charged particle faces. The random assembly of multiple aggregates constitutes macro-
167 scale structures. Several studies, such as those of Alonso et al. (1987), Lloret et al. (2003) and
168 Delage et al. (2006), analyzed the pore size distribution in expansive clays compacted by fol-
169 lowing the approach of block fabrication. Their results showed, that the total pore space is com-
170 prised of different kinds of pore populations at different scales, being characterized by a bi-
171 modal-shaped pore size distribution curve. Interlayer spaces are planar void spaces between the
172 unit layers, while the inter-particle pores are present between particles and inside aggregates.
173 Randomly arranged aggregates account for the inter-aggregate pores. The latter two pore pop-
174 ulations are referred to as micro-pores and macro-pores. Increasing dry densities cause a sig-
175 nificant reduction in the macro-porosity, while the micro-porosity remains stable. Overlapping
176 repulsive forces contribute to the conservation of micro-porosity (Lloret et al., 2003).

177 The exponential relation of the initial dry density and the maximum values of the swelling
178 pressure and free swell strains were determined in several studies (Komine et al., 2009; Schanz
179 and Tripathy, 2009; Baille et al., 2010). The mentioned literature elaborately informs about the
180 approaches adopted to explain this exponential relation.

181 This experimental program quantified the enhancement of the swelling behavior attaina-
182 ble by mixing $COX_c$ with bentonite. The obtained results were complemented by information

183 regarding the contribution of expansive mineral phases in $COX_c$ to the maximum swelling pres-
184 sure of mixtures. Moreover, the experiments aimed to determine, whether the swelling behavior
185 of $COX_c$ and its mixtures is more susceptible to variations in initial dry density or saturating
186 solution chemistry, since information about their impact is scarcely available. A comprehensive
187 platform was provided by these means, permitting to assign the observations to the single and
188 combined impacts.

## 189 3 Materials

190 COX-claystone was obtained by excavating drifts of ANDRA URL in Bure at a depth of
191 – 490 m. A few weeks afterwards, the excavated material was industrially crushed to maximum
192 grain sizes of 2.00 mm and filled into sealed barrels. According to Robinet et al. (2012) and
193 Conil et al. (2018), the mineralogical composition, initial water content and initial porosity of
194 COX-claystone vary depending on the location in the sedimentary layer. COX-claystone is
195 composed of 20 – 60% clay minerals being dominated by illite and interstratified illite/ smec-
196 tite, 10 – 40% quartz and feldspars, 15 – 80% carbonates, and low amounts of pyrites. In con-
197 trast to intact drill cores of COX-claystone, whose initial water content are approximately 8.0%
198 (Conil et al., 2018), the water content of $COX_c$ was 5.4%. This decrease was attributed to the
199 crushing process and the duration of the storage. MX80-bentonite (Wyoming, USA) was se-
200 lected to be mixed with $COX_c$, since it exhibits beneficial material properties, especially re-
201 garding its high volume change, low conductivity and high retention behavior (Pusch, 1992).
202 Like $COX_c$, it was industrially crushed to maximum grain diameters of 0.28 mm and 2.00 mm,
203 and filled by the supplier (Laviosa-MPC SAS, Limay, France) into sealed buckets. Information
204 regarding the approximated mineralogical composition of the employed MX80-bentonite is
205 given in Table 1. The water content, liquid limit, plastic limit and specific gravity of $COX_c$ and

206 the mixtures were determined following the French standard (AFNOR, 1991, 1993). The deter-
207 mined physical properties of $COX_c$ and the mixtures are compiled in Table 2. The correspond-
208 ing values of MX80-bentonite are provided for the purpose of comparison.
209 The grain size distribution curves were obtained in two steps. First, grains larger than
210 0.80 mm in diameter were separated from the finer fractions via dry sieving. Since the bentonite
211 fraction in the mixtures was expected to clog the finer meshes when coming into contact with
212 water, the method of dry sieving was favored over wet sieving. The grain size distribution of
213 the finer fractions was measured via laser diffractometry, following ISO (2009). The obtained
214 distribution curves are depicted in Figure 1. The replacement of $COX_c$ by bentonite with a
215 maximum grain size of 0.28 mm caused a shift in the distribution curve to higher values, cor-
216 responding to a general increase in the amount of fines in the powder mixture.
217 Sample preparation, as well as standard and modified Proctor tests, were conducted ac-
218 cording to the French standard (AFNOR, 2014). The materials were prepared in a mechanical
219 mixer at various molding water contents and filled in plastic bags after termination of the mix-
220 ing process. Various molding water contents were established by adding deaired/ demineralized
221 water to the original materials. The bags were then stored under ambient room conditions (T =
222 20 ± 2°C). During a period of one week, the plastic bags were frequently revolved to guarantee
223 a homogeneous water content distribution. The results of the standard and modified Proctors
224 tests performed on $COX_c$ and the mixtures are depicted in Figure 2 a and b. The replacement of
225 $COX_c$ reduced the maximum dry density considerably and shifted the optimum water contents
226 to higher values, regardless of the applied compaction energy. In the case of compacting the
227 mixtures by using standard compaction energy, the impact of an increasing water content on
228 the dry density at the dry side of the optimum water content was negligible.
229 Three different aqueous solutions, namely, deionized/ demineralized water (DW), artifi-
230 cial Bure site solution (ABSS) and artificial Portland cement solution (APCS), were employed.

They varied in their chemical compositions, ionic strengths and pH values. DW represented the reference case, since its chemical composition was expected to not affect the material behavior, while ABSS and APCS were believed to alter the swelling behavior as the site water at a depth of – 490 m and the occurring hyperalkaline solution, respectively. Both solutions were prepared according to information given by ANDRA. The compounds, main ion species and other characteristics of ABSS and APCS are compiled in Table 3.

# 4 Methods

The materials were prepared following the previously established protocol (Section 3). The samples were envisaged to be compacted to maximum dry densities (± 1%) at individual optimum water contents (± 1%), as determined in modified Proctor tests. Variations in the initial dry density were portrayed by reducing the maximum dry density of samples by 2.5%, 7.5% and 17.5%, while keeping the optimum water content. In the following, coefficients of dry density reduction were indicated by $R_{\rho d,\,max}$. Although it must be assumed that values of the initial dry density were shifted to the dry side of the compaction curve by reducing the maximum dry density and keeping the optimum water content, the approach was believed to adequately portray the conditions in situ. The reduction of the initial dry density by 17.5% with respect to the maximum dry density, for instance, corresponds to a loss of compaction energy of approximately 20%. Such a loss of compaction energy is likely to occur, if the materials are compacted close to the drift wall or the drift top. Conversely, the preparation of backfill materials to their optimum water contents and their conservation were less challenging tasks in situ (Gunnarson et al., 2001).

The samples were compacted statically to target dry densities at a controlled rate of 0.1 mm/s inside the rings. The initial dimensions of each sample were 15 mm in height and 70 mm in diameter. By compacting the samples directly inside the rings, the risk of creating

preferential flow paths and, in turn, saturating the samples heterogeneously, was significantly reduced. The ring, which contained the compacted sample being sandwiched between two porous discs, was screwed to the lid and the bottom plate. Then, the assembled cell was positioned in a load frame and the bottom plate was connected to a volume-/ pressure control unit, enabling the saturation of the sample with a given pressure from the bottom of the cell upwards. A graduated flask was used to collect the outflowing solution. The load frame was equipped with an external load sensor, an internal load sensor, and a linear transducer. The linear transducer monitored the vertical position of the piston. Detecting an upward movement that was triggered by material swelling, the load frame automatically adapted the position of the piston downwards. By these means, the volume was kept constant. The evolving swelling pressure was recorded by two load sensors.

First, the experiment protocol envisaged to subject the samples to a vertical stress equal to 10 kPa. This approach served the purpose of establishing a good contact between the bottom plate, the porous disks, the sample, and the piston. The load frame kept the position of the piston constant afterwards. The bottom plate was flushed before imposing the injection pressure of 15 kPa, corresponding to a hydraulic gradient of 100, considering a sample height of 15 mm. By these means, the residual air in the bottom plate was removed. The swelling pressure experiments were stopped after 10 000 minutes (≈ 7 days). Detailed information about the samples and their major initial characteristics are given in the first part of the supplementary materials.

## 5 Results

The constant-volume swelling pressure experiments aimed to investigate the impact of replacing 30% of $COX_c$ with bentonite on the short-term evolution of the swelling pressure of $COX_c$ and the mixtures. The complementing experiments analyzed the response of the swelling pressure to variations in the dry density, as well as the saturating solution chemistry.

279 The evolutions of the swelling pressure of $COX_c$ and the mixtures are depicted in Fig-
280 ure 3. Materials being compacted using higher energies generally exhibited higher swelling
281 pressures. The maximum swelling pressures of $COX_c$ and the grain-mixture were comparably
282 low, while the powder-mixture was characterized by slightly elevated pressures, if it was com-
283 pacted using standard energy. The maximum swelling pressure of the powder-mixture was
284 990 kPa, corresponding to an increase by 30% and 65%, compared to the maximum values of
285 the grain-mixture and $COX_c$, respectively.

286 Generally identified, the mixtures reacted to variations in solution chemistry less suscep-
287 tibly than $COX_c$, when being compacted to maximum dry densities at optimum water contents.
288 The impact of variations in the solution chemistry was thus more pronounced in the case of
289 $COX_c$. The comparison of the material response is depicted in Figure 4. It became evident that
290 the alkaline solution impaired the material performance more significantly than ABSS, alt-
291 hough it had a lower ionic strength. For instance, the saturation with ABSS reduced the maxi-
292 mum swelling pressure by 6% in the case of the grain mixture and by 44% in case of $COX_c$.
293 The grain-mixture lost 13% of its maximum swelling pressure, while a loss of 69% was meas-
294 ured upon bringing $COX_c$ in contact with APCS.

295 The reduction in the dry density caused a significant loss in the swelling pressure in the
296 individual experiments, when compacting the material at optimum water content. The impact
297 of the reduced dry densities in the case of the grain-mixture is presented in Figure 5. Accord-
298 ingly, maximum values were determined at the highest dry densities. A reduction of 2.5%, 7.5%
299 and 17.5% decreased the maximum swelling pressure by 20%, 65% and 85%, respectively.
300 Moreover, the material saturation accelerated as the dry density decreased. The reduction in the
301 maximum dry density and the maximum swelling pressure of both mixtures were exponentially
302 related (Figure 6 a and b). The corresponding regression line is given by the equation:

$$\sigma_s = \sigma_{s,max} \exp(-\beta R_{\rho_{d,max}}) \quad (5.1)$$

where $\sigma_{s,\,max}$ is the highest expectable swelling pressure and $\beta$ is the slope indicating the swelling pressure decrease with the dry density reduction. As already identified, even a reduction in the material dry density of 2.5% provoked a significant decrease of swelling pressure, regardless of the mixture and the saturating solution chemistry. The values of the $\beta$-parameters of grain- and powder-mixtures were in the same range, indicating a similar impact of the solution chemistry on the short-term material performance. However, the values were smaller compared to the others, in the case of the $\beta$-parameters of ABSS.

The major results of the performed swelling pressure experiments are compiled in the second part of the supplementary materials. Information about the major final characteristics of samples are added. The expansive mineral dry density (EDD) will be introduced in section 6.1.

# 6 Discussion

Most of obtained results are neither comparable nor interpretable with relations that are presented in the literature, since the reduction in the maximum dry density $R_{\rho d,\,max}$ represents a value being relative to the individual maximum dry density. Thus, replacing the reduction by a generally more applicable variable might be recommended. Section 6.1 briefly introduces the expansive material dry density (EDD) and its major purpose, while the following sections discuss the obtained results.

## 6.1 Introduction of expansive mineral dry density (EDD)

$COX_c$ and MX80-bentonite are referred to as expansive materials that are generally composed of expansive and inert mineral phases. Results of constant-volume swelling pressure experiments performed on $COX_c$ suggested a non-negligible contribution of the expansive mineral phases in $COX_c$ to the maximum swelling pressure of mixtures (Figure 3). It was thus assumed that the total fraction of the expansive mineral phases must account for the swelling character-

istics of mixtures. Concepts such as the bentonite dry density attributing the behavior of mixtures of bentonite and non-expansive materials only to the bentonite fraction (Bucher and Jedelhauser, 1985; Villar and Rivas, 1994; Dixon, 2000; Agus and Schanz, 2008; Wang et al., 2012) were hardly applicable in the case of claystone/ bentonite mixtures, as they disregard expansive mineral phases in $COX_c$ on the one hand and inert mineral phases in MX80-bentonite on the other hand. Unlike the approach of Zeng et al. (2019) which considered the contribution of expansive mineral phases in $COX_c$ to material swelling of bentonite/ claystone mixtures by introducing an inhibition factor, the expansive mineral dry density (EDD) was aimed at relating the swelling characteristics of bentonites and their mixtures to their mineralogical composition. Apart from attributing material swelling to the total fraction of the expansive mineral phases in the mixtures, the following assumptions are also considered prior to its employment. The pore water being present is exclusively attached to the expansive mineral phases; the porosity of the fraction of inert mineral phases is so low that expansive mineral phases occupy the entire macro-pore space when they swell; and material compaction only causes a reduction in the macro-pore space.

In the following, materials containing expansive mineral phases are classified into the expansive and inert mineral phases, as well as the fluid phase and the gas phase. The corresponding phase diagram is depicted in Figure 7. The total fraction of expansive mineral phases in the mixtures was calculated by first summing the fraction of expansive mineral phases ($x_{ji}$) in each material ($i$) up and then multiplying the obtained sum by the total fraction of the corresponding material in the mixture ($f_i$). The results of the second step were then summarized to consider all materials in the mixture. The total fraction of inert mineral phases in the mixtures was calculated similarly. For instance, the total fraction of smectite in the mixture was calculated by first multiplying 0.83 (Table 1) representing the fraction of smectite in MX80-bentonite by 0.3 representing the fraction of MX80-bentonite in the mixture. The fraction of smectite in

$COX_c$ was assumed to be equal to 0.15 as $COX_c$ only contains fractions of interstratified illite/smectite. Its multiplication by 0.7 makes the fraction of smectite in $COX_c$. The final value of the fraction of smectite in the mixture is obtained by summing 0.25 and 0.15 up being equal to 0.35. EDD was defined as the ratio of the dry mass of the total fraction of expansive mineral phases in the mixture to the combined volume of the total fraction of expansive mineral phases in the mixture and the pore volume. The denominator of the ratio is substitutable by the difference between the total volume of the mixture and the volume of the total fraction of inert mineral phases in the mixture. EDD is given as:

$$EDD = \left[\sum_i \sum_j f_i \, x_{ji}\right]\left[\frac{1}{\rho_d} - \left(\frac{1 + w_{ini}}{\rho_w}\right)\left[\sum_i \sum_k \frac{f_i \, y_{ki}}{G_{s\,ki}}\right]\right]^{-1} \tag{6.1}$$

where $f_i$ is the mass fraction of material $i$ in the mixture, $x_{ji}$ is the mass fraction of expansive mineral phase $j$ in material $i$, $y_{ki}$ is the mass fraction of inert mineral phase $k$ in material $i$ and $G_{s\,ki}$ is the specific gravity of the inert mineral phase $k$ in the material $i$. For instance, the calculation of the mass fraction of smectite in the investigated mixtures proceeds as follows: The mass fraction of MX80-bentonite in the mixture is initially multiplied by the mass fraction of smectite in MX80-bentonite. Similarly, the mass fraction of smectite in $COX_c$, which is present in the mixture, is calculated in the next step. The sum of both multiplications eventually gives the mass fraction of smectite in the investigated mixtures.

The equation is complemented by the dry density of the mixture ($\rho_d$), the density of the water ($\rho_w$), and the initial water content of the mixture ($w_{ini}$). Its utilization allowed a comparison of the impact of densification on the maximum swelling pressure of not only the bentonites being predominantly composed of expansive minerals, such as MX80-bentonite, but also mixtures of those bentonites with less- and non-expansive materials, such as $COX_c$ or sand.

## 6.2 Impact of expansive mineral content and grain size distribution

First, the impact of $COX_c$-replacement by bentonite on the compaction and swelling properties was assessed. Comparing the compaction curves of $COX_c$ and both mixtures, $COX_c$ exhibited a significantly higher compactitibility, indicated by the higher dry densities (Figure 2). The compaction behavior of the mixtures was alike that of pure MX80-bentonite, since varying water contents had a minor impact on the attained dry densities at the dry side of the compaction curve (Dixon et al., 1985). These findings were complemented by Pusch (1995), Keto et al. (2006) and this study. They observed a more pronounced sensitivity of material dry density to varying water content and compaction energy with a lower amount of expansive material in the mixture. Dixon et al. (1985) related the observed insensitivity of MX80-bentonite to the higher viscosity of adsorbed water on clay particles, which induces an elevated shear strength. This resistance might be higher than the applied compaction energies. Consequently, the shear strength might decrease with an increasing amount of less- or non-expansive material. As described by Komine and Ogata (1999), an increasing fraction of expansive material in these mixtures provokes higher swelling pressures, if compacted to maximum dry density at optimum water content.

Referring to the impact of the amount of fines on the compaction and swelling properties, it became evident that the powder-mixture exhibited a higher compactability than the grain-mixture when compacting it by using the modified compaction energy. The measured swelling pressures of the powder-mixture were higher than those of the grain-mixture due to the higher dry density and the lower optimum water content. Keto et al. (2006) performed modified Proctor experiments on crushed granite rock/ bentonite-mixtures. According to their findings, the highest dry densities can be attained by employing materials having the widest grain size distribution and the highest amount of fines. A wider grain size distribution provokes a denser packing of particles and, in turn, reduces the amount of macro-porosity.

## 6.3 Individual impact of EDD and solution chemistry

The introduction of EDD aimed to compare the impact of densification on any material that contains fractions of expansive minerals. Its applicability was verified by calculating EDD derived from different literature and plotting the values against the reported maximum swelling pressures. The obtained results compared to the literature data are depicted in Figure 8. The comparison affirmed the significance of EDD as one key variable governing the maximum swelling pressure of materials containing expansive mineral phases. The grain- and powder-mixtures reacted to elevated EDD with increasing swelling pressures as depicted in Figure 8. According to section 2, these results were most likely attributable to the higher probability of double layer repulsion. The exponential relationship of EDD and the maximum swelling pressure of each bentonite, including its mixtures, seemed to be unique although this issue has not been confirmed. This trend was particularly noticeable by comparing the slope of the individual regression lines of the materials composed of MX80-bentonite. The general trend can be approximated by the following generalized equation of the regression curve:

$$\sigma_{s,max} = \sigma_{s,min} \exp(\beta^* EDD) \tag{6.2}$$

where $\sigma_{s,\,min}$ can be considered to be the minimal swelling pressure that is theoretically evolving, if the material is in a loose state, while $\beta^*$ identifies the actual impact of varying EDD on the maximum swelling pressure. Apart from the initial dry density and the initial water content, the $\beta^*$ parameter is predominantly controlled by the mass fraction of expansive minerals in the material. This finding is consistent, as EDD might increase with a higher mass fraction of expansive mineral phases at the same dry density. Table 4 gives information about the different values of $\sigma_{s,\,min}$ and $\beta^*$.

$COX_c$, the grain- and powder-mixtures were characterized by initial suctions of 1.5 MPa, 2.9 MPa and 4.3 MPa, respectively, when the samples were compacted to the maximum dry

density at their individual water content by using modified compaction energy. These initial suctions suggest that osmotic swelling might more contribute to the development of swelling pressure under constant-volume conditions than crystalline swelling. As the magnitude of osmotic swelling is susceptible to the saturating solution chemistry, particularly the cations in solution and the ionic strength, the swelling pressures of $COX_c$ and the mixtures were expected to be affected by the employed solution. Interestingly, such an impact was observed only in the case of $COX_c$ whereas both mixtures hardly reacted to the different solutions. The higher susceptibility of $COX_c$ cannot be reasonably explained yet, thus demanding more investigations.

## 6.4 Combined impact of solution chemistry and EDD

Comparable to this study, some studies also emphasized the impact of variations in the ionic strength of solutions on the swelling pressure of different bentonites that were compacted to different dry densities (Pusch, 1980; Karnland, 1997; Dixon, 2000; Pusch, 2001; Castellanos et al., 2008; Komine et al., 2009; Xiang et al., 2019). Generally, the impact of the ion concentration is more pronounced in the case of less compacted bentonites. The observed effect vanishes as the dry density and montmorillonite content increase.

Conversely, the different saturating solutions had a minor impact on the maximum swelling pressure of the grain- and powder-mixtures, even when the samples were compacted to lower values of EDD. This finding can be deduced from $\sigma_{s,\,min}$ and $\beta^*$ parameters in Figure 9 a and b, despite the grain-mixture saturated with ABSS exhibited a greater deviation of those parameters. Most probably, the low concentration of cations in solution caused an only partial exchange of cations hardly affecting the thickness of diffuse double layers and in turn the maximum swelling pressure of the grain- and powder-mixtures.

# 7 Conclusions

The current laboratory experimental program assessed the impact of partly replacing crushed COX-claystone ($COX_c$) with MX80-bentonite on the compaction and on the swelling behavior of mixtures that could potentially be employed to backfill drifts and shafts of a future repository for nuclear waste in deep sedimentary rock formations. Complementary experiments investigated the impact of variations in the dry density and saturating solution chemistry on the evolution of the swelling pressure. The reference concept envisages the employment of conventional compaction techniques to install the backfill directly inside the drifts and shafts. The considered backfill materials are composed of 70 % crushed COX-claystone ($COX_c$) and 30 % MX80-bentonite grains or powder in wet mass. $COX_c$ served as a reference material to identify the impact of the material replacement. Evolving swelling pressures were determined by means of the constant-volume method. The employed samples were then prepared to maximum and reduced dry densities at optimum water contents, which were obtained in modified Proctor tests. The samples were saturated with three solutions, greatly varying in pH values and ionic strengths. The following conclusions can be drawn from the laboratory experimental program:

1) The replacement of 30% $COX_c$ by either MX80-bentonite grains or powder caused a shift in the maximum dry density to lower values and of the optimum water content to higher values, regardless of the applied compaction energy. Compared to the grain-mixture, the powder-mixture exhibited a higher maximum dry density at a lower initial water content when compacting using the same energy. This finding was attributed to an optimized particle packing caused by a higher amount of fines. The maximum swelling pressure of both mixtures was higher than that of $COX_c$, despite the lower maximum dry density. Generally, these finding were in accordance with the literature, as the amount of expansive minerals phases in the mixtures was higher.

2) The swelling pressure of the claystone/ bentonite mixtures was identified as being hardly affected by the saturating solution chemistry, when compacting both mixtures to their maximum dry densities at optimum water contents. This might be caused by the low ionic strength of the employed solutions. The swelling pressure of $COX_c$ seemed to be more susceptible to the saturating solution chemistry. More experiments are required to adequately explain this point. Generally applicable, expansive mineral dry density (EDD) improved the comparability of the impact of densification on the swelling pressure of materials that contain fractions of expansive mineral phases. Its introduction was claimed by the considerable contribution of expansive mineral phases in $COX_c$ to material swelling. The exponential relationship of EDD and the maximum swelling pressure was identified as being unique in the cases of every bentonite and its mixtures.

3) In the case of the grain-and powder-mixture, the different saturating solutions had a minor impact on the maximum swelling pressure of the grain- and powder-mixtures, even when the samples were compacted to lower values of EDD. This finding can be predominantly attributed to the low concentration of cations in solution and the low ionic strength of the employed saturating solutions.

It is recommended that MX80-bentonite powder-based mixtures are favored over grain-mixtures if employing conventional compaction techniques to install backfill in drifts and shafts, as higher short-term swelling pressures can be attained. It became evident that varying dry densities affect the material performance of the claystone/ bentonite mixtures more significantly than potential environmental conditions. Thus, high demands must be made on the quality management during backfill installation. Generally, this study improved the knowledge about mixtures of the materials each containing expansive mineral phases in terms of their compaction and swelling behavior. Future studies will assess the long-term evolution of the material

behavior of grain- and powder-mixtures, especially the swelling pressure and hydraulic conductivity. It is also of interest to investigate the material behaviors under varying degrees of saturation.

## Acknowledgement

The authors gratefully thank Dr. G. Armand, Dr. N. Michau and Dr. J. Zghondi of ANDRA for fruitful discussions. The authors also wish to thank the editor and the reviewers for helpful comments on the manuscript.

## Funding

This research did not receive any specific grant from funding agencies in the public, commercial, or not-for-profit sectors.

# References


AFNOR, 1991. Soils: Investigation and testing: Determination of particle density - Pycnometer method. Association Francaise de Normalisation (AFNOR).

AFNOR, 1993. Soils: Investigation and testing: Determination of Atterberg's limits -Liquid limit test using Casagrande apparatus - Plastic limit test on rolled thread. Association Francaise de Normalisation (AFNOR).

AFNOR, 2014. Soils: Investigation and testing: Determination of the compaction reference values of a soil type - Standard Proctor Test - Modified Proctor Test. Association Francaise de Normalisation (AFNOR).

Agus, S.S., Schanz, T., 2008. A method for predicting swelling pressure of compacted bentonites. Acta Geotech. 3, 125–137. 10.1007/s11440-008-0057-0.

Alonso, E.E., Gens, A., Whight, D.W., 1987. General Report, in: Groundwater effects in geotechnical engineering. Ninth european conference on soil mechanics and foundation engineering, Dublin. 31.08. - 03.09. A. A. Balkema, Rotterdam, Brookfield, pp. 1087–1146.

Andra, 2005. Dossier 2005 Argile - Synthesis: Evaluation of the feasibility of a geological repository in an argillaceous formation (Meuse/ Haute-Marne Site). French National Radioactive Waste Management Agency, Chatenay-Malabry CEDEX, 241 pp. Accessed 22 November 2018.

Baille, W., Tripathy, S., Schanz, T., 2010. Swelling pressures and one-dimensional compressibility behaviour of bentonite at large pressures. Applied Clay Science 48, 324–333. 10.1016/j.clay.2010.01.002.

Bolt, G.H., 1956. Physico-chemical analysis of the compressibility of pure clays. Géotechnique 6, 86–93.

523 Bradbury, M.H., Baeyens, B., 2003. Porewater chemistry in compacted re-saturated MX-80
524 bentonite. Journal of Contaminant Hydrology 61, 329–338. 10.1016/S0169-
525 7722(02)00125-0.
526 Bucher, F., Jedelhauser, P., 1985. Verdichtungsversuche an Quarzsand-Bentonit-Gemischen.
527 Technischer Bericht 85-52. National Cooperative for the Disposal of Radioactive Waste,
528 Zuerich, 25 pp. Accessed 25 February 2019.
529 Castellanos, E., Villar, M.V., Romero, E., Lloret, A., Gens, A., 2008. Chemical impact on the
530 hydro-mechanical behaviour of high-density FEBEX bentonite. Physics and Chemistry of
531 the Earth, Parts A/B/C 33, S516-S526. 10.1016/j.pce.2008.10.056.
532 Chen, F.H., 1988. Foundations on expansive soils. Elsevier science pub, Amsterdam, New
533 York, 1463 pp.
534 Conil, N., Talandier, J., Djizanne, H., La Vaissière, R. de, Righini-Waz, C., Auvray, C., Mor-
535 lot, C., Armand, G., 2018. How rock samples can be representative of in situ condition: A
536 case study of Callovo-Oxfordian claystones. Journal of Rock Mechanics and Geotechnical
537 Engineering 10, 613–623. 10.1016/j.jrmge.2018.02.004.
538 Cuisinier, O., Deneele, D., Masrouri, F., 2009. Shear strength behaviour of compacted clayey
539 soils percolated with an alkaline solution. Engineering Geology 108, 177–188.
540 10.1016/j.enggeo.2009.07.012.
541 Cuisinier, O., Deneele, D., Masrouri, F., Abdallah, A., Conil, N., 2014. Impact of high-pH
542 fluid circulation on long term hydromechanical behaviour and microstructure of com-
543 pacted clay from the laboratory of Meuse-Haute Marne (France). Applied Clay Science
544 88-89, 1–9. 10.1016/j.clay.2013.12.008.
545 Delage, P., Marcial, D., Cui, Y.J., Ruiz, X., 2006. Ageing effects in compacted bentontie: A
546 microstructure approach. Géotechnique 56, 291–304.

547 Dixon, D.A., 2000. Porewater salinity and the development of swelling pressure in bentonite-
548 based buffer and backfill materials. POSIVA 2000-04. POSIVA Oy, Helsinki, 51 pp. Ac-
549 cessed 13 November 2019.
550 Dixon, D.A., Gray, M.N., Thomas, A.W., 1985. A study of the compaction properties of po-
551 tential clay—sand buffer mixtures for use in nuclear fuel waste disposal. Engineering Ge-
552 ology 21, 247–255. 10.1016/0013-7952(85)90015-8.
553 Gens, A., Alonso, E.E., 1992. A framework for the behaviour of unsaturated expansive clays.
554 Can. Geotech. J. 29, 1013–1032. 10.1139/t92-120.
555 Gunnarson, D., Börgesson, L., Hökmark, H., Johannesson, L.-E., Sandén, T., 2001. Äspö
556 Hard Rock Laboratory: Installation of the Backfill and Plug test. International Progress
557 Report 01-17. Swedish Nuclear Fuel and Waste Management Co, Stockholm, 236 pp. Ac-
558 cessed 20 November 2018.
559 Herbert, H.-J., Kasbohm, J., Moog, H.C., Henning, K.-H., 2004. Long-term behaviour of the
560 Wyoming bentonite MX-80 in high saline solutions. Applied Clay Science 26, 275–291.
561 10.1016/j.clay.2003.12.028.
562 ISO, 2009. Particle size analysis: Laser diffraction methods.
563 Johannesson, L.-E., 2014. Prototype Repository: Measurements of water content and density
564 of the retrieved buffer material from deposition hole 5 and 6 and the backfill in the outer
565 section of the Prototype Repository. P-13-14. Swedish Nuclear Fuel and Waste Manage-
566 ment Co, Stockholm, 180 pp. Accessed 8 February 2019.
567 Karnland, O., 1997. Bentonite swelling pressure in strong NaCl solutions – Correlation be-
568 tween model calculations and experimentally determined data. Technical Report 97-31.
569 Swedish Nuclear Fuel and Waste Management Co, Stockholm, 40 pp. Accessed 21 No-
570 vember 2018.

571 Karnland, O., Olsson, S., Nilsson, U., Sellin, P., 2007. Experimentally determined swelling
572 pressures and geochemical interactions of compacted Wyoming bentonite with highly al-
573 kaline solutions. Physics and Chemistry of the Earth, Parts A/B/C 32, 275–286.
574 10.1016/j.pce.2006.01.012.
575 Keto, P., Kuula-Vaeisaenen, P., Ruuskanen, J., 2006. Effect of Material Parameters on the
576 Compactibility of Backfill Materials. Working Report 2006-34. POSIVA Oy, Olkiluoto.
577 Komine, H., Ogata, N., 1999. Experimental study on swelling characteristics of sand-benton-
578 ite mixture for nuclear waste disposal. Soils and Foundation 39, 83–97.
579 Komine, H., Yasuhara, K., Murakami, S., 2009. Swelling characteristics of bentonites in arti-
580 ficial seawater. Canadian Geotechnical Journal 46, 177–189. 10.1139/T08-120.
581 Lloret, A., Villar, M.V., Sanchez, M., Gens, A., Pintado, X., Alonso, E.E., 2003. Mechanical
582 behaviour of heavily compacted bentonite under high suction changes. Géotechnique 53,
583 27–40. 10.1680/geot.53.1.27.37258.
584 Madsen, F.T., Müller-Vonmoos, M., 1989. The swelling behaviour of clays. Applied Clay
585 Science 4, 143–156. 10.1016/0169-1317(89)90005-7.
586 Mitchell, J.K., Soga, K., 2005. Fundamentals of soil behavior, 3rd ed. Wiley, Hoboken, N.J.,
587 Chichester.
588 Müller-Vonmoos, M., Kahr, G., 1983. Mineralogische Untersuchungen von Wyoming-
589 Bentonit MX-80 und Montigel. Technical Report 83-12. National Cooperative for the Dis-
590 posal of Radioactive Waste, Zuerich, 37 pp. Accessed 17 January 2019.
591 Pusch, R., 1980. Swelling pressure of highly compacted bentonite. Technical Report 80-13.
592 Swedish Nuclear Fuel and Waste Management Co, Stockholm, 35 pp. Accessed 23 No-
593 vember 2018.
594 Pusch, R., 1992. Use of bentonite for isolation of radioactive waste products. Clay miner. 27,
595 353–361. 10.1180/claymin.1992.027.3.08.

596 Pusch, R., 1995. Consequences of using crushed crystalline rock as ballast in KBS-3 tunnels
597 instead of rounded quartz particles. Technical Report 95-14. Swedish Nuclear Fuel and
598 Waste Management Co, Stockholm, 51 pp. Accessed 26 February 2019.
599 Pusch, R., 2001. Experimental study of the effect of high porewater salinity on the physical
600 properties of a natural smectitic clay. Technical Report 01-07. Swedish Nuclear Fuel and
601 Waste Management Co, Stockholm, 32 pp. Accessed 21 November 2018.
602 Pusch, R., Yong, R., 2003. Water saturation and retention of hydrophilic clay buffer—micro-
603 structural aspects. Applied Clay Science 23, 61–68. 10.1016/S0169-1317(03)00087-5.
604 Pusch, R., Zwahr, H., Gerber, R., Schomburg, J., 2003. Interaction of cement and smectitic
605 clay—theory and practice. Applied Clay Science 23, 203–210. 10.1016/S0169-
606 1317(03)00104-2.
607 Robinet, J.-C., Sardini, P., Coelho, D., Parneix, J.-C., Prêt, D., Sammartino, S., Boller, E.,
608 Altmann, S., 2012. Effects of mineral distribution at mesoscopic scale on solute diffusion
609 in a clay-rich rock: Example of the Callovo-Oxfordian mudstone (Bure, France). Water
610 Resources Research 48, 819. 10.1029/2011WR011352.
611 Schanz, T., Tripathy, S., 2009. Swelling pressure of a divalent-rich bentonite: Diffuse double-
612 layer theory revisited. Water Resources Research 45, 1752. 10.1029/2007WR006495.
613 Sridharan, A., Choudhury, D., 2002. Swelling pressure of sodium montmorillonites. Géotech-
614 nique 52, 459–462. 10.1680/geot.2002.52.6.459.
615 Sridharan, A., Rao, A.S., Sivapullaiah, P.V., 1986. Swelling Pressure of Clays. Geotechnical
616 Testing Journal 9, 24–33. 10.1520/GTJ10608J.
617 Tang, C.S., Tang, A.M., Cui, Y.J., Delage, P., Schroeder, C., Laure, E. de, 2011a. Investigat-
618 ing the swelling pressure of compacted crushed-Callovo-Oxfordian claystone. Physics and
619 Chemistry of the Earth, Parts A/B/C 36, 1857–1866. 10.1016/j.pce.2011.10.001.

620 Tang, C.S., Tang, A.M., Cui, Y.J., Delage, P., Schroeder, C., Shi, B., 2011b. A study of the
621 hydro-mechanical behaviour of compacted crushed argillite. Engineering Geology 118,
622 93–103. 10.1016/j.enggeo.2011.01.004.
623 Tang, C.S., Tang, A.M., Cui, Y.J., Delage, P., Shi, B., 2010. The coupled hydro-mechanical
624 behaviours of compacted crushed Callovo-Oxfordian argillite. Journal of Rock Mechanics
625 and Geotechnical Engineering, 86–90.
626 Tombácz, E., Szekeres, M., 2004. Colloidal behavior of aqueous montmorillonite suspen-
627 sions: the specific role of pH in the presence of indifferent electrolytes. Applied Clay Sci-
628 ence 27, 75–94. 10.1016/j.clay.2004.01.001.
629 Tombácz, E., Szekeres, M., 2006. Surface charge heterogeneity of kaolinite in aqueous sus-
630 pension in comparison with montmorillonite. Applied Clay Science 34, 105–124.
631 10.1016/j.clay.2006.05.009.
632 van Olphen, H., 1977. An introduction to clay colloid chemistry: For clay technologists, geol-
633 ogists, and soil scientists, 2nd ed. Wiley, New York (N.Y.), 1318 pp.
634 Villar, M.V., Rivas, P., 1994. Hydraulic properties of montmorillonite-quartz and saponite-
635 quartz mixtures. Applied Clay Science 9, 1–9. 10.1016/0169-1317(94)90011-6.
636 Wang, Q., Cui, Y.J., Tang, A.M., Delage, P., Gatmiri, B., Ye, W.M., 2014. Long-term effect
637 of water chemistry on the swelling pressure of a bentonite-based material. Applied Clay
638 Science 87, 157–162. 10.1016/j.clay.2013.10.025.
639 Wang, Q., Tang, A.M., Cui, Y.J., Delage, P., Gatmiri, B., 2012. Experimental study on the
640 swelling behaviour of bentonite/claystone mixture. Engineering Geology 124, 59–66.
641 10.1016/j.enggeo.2011.10.003.
642 Xiang, G., Xu, Y., Yu, F., Fang, Y., Wang, Y., 2019. Prediction of swelling characteristics of
643 compacted GMZ bentonite in salt solution incorporating ion-exchange reactions. Clays
644 Clay Miner. 67, 163–172. 10.1007/s42860-019-00014-3.

645 Yong, R.N., 1999. Soil suction and soil-water potentials in swelling clays in engineered clay
646 barriers. Engineering Geology 54, 3–13. 10.1016/S0013-7952(99)00056-3.
647 Zeng, Z., Cui, Y.J., Zhang, F., Conil, N., Talandier, J., 2019. Investigation of swelling pres-
648 sure of bentonite/claystone mixture in the full range of bentonite fraction. Applied Clay
649 Science 178, 105137. 10.1016/j.clay.2019.105137.

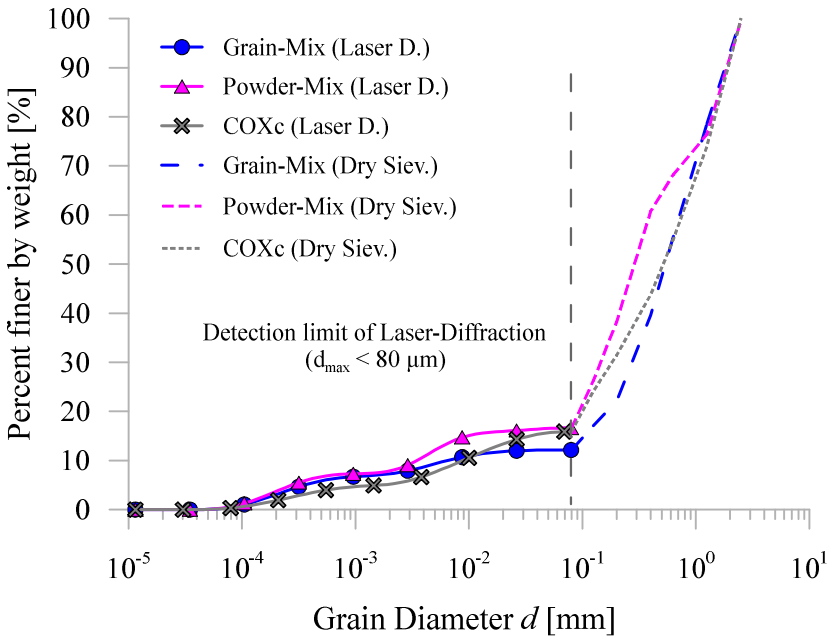


Figure 1: Grain size distribution curves of COXc, grain- and powder-mixtures obtained by dry sieving and laser diffractometry

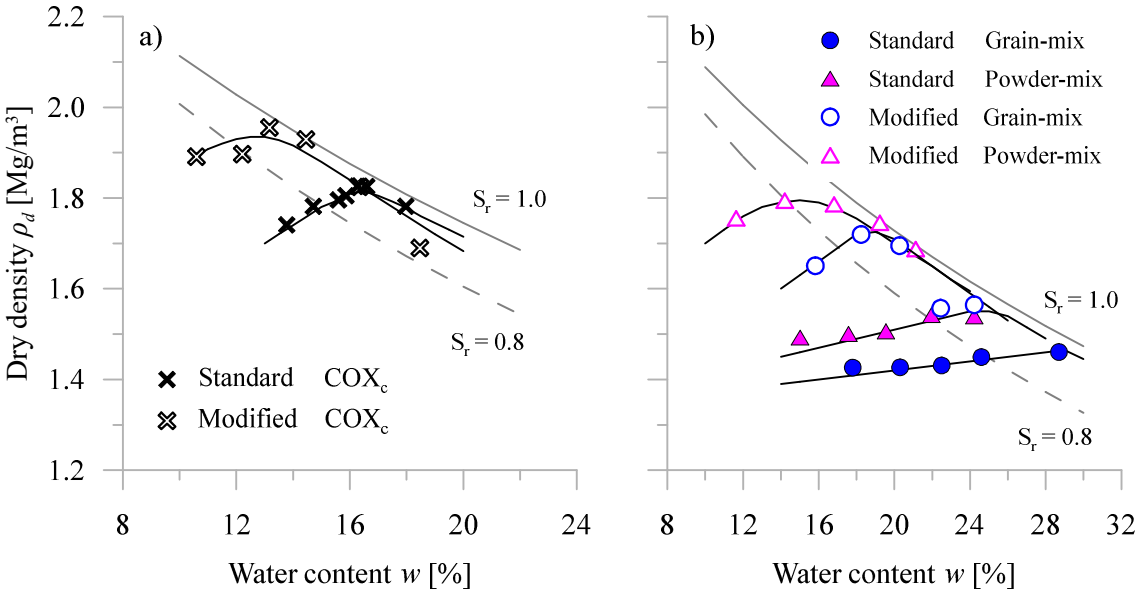


Figure 2: a) Results of the standard and modified Proctor tests performed on COXc, b) Results of the standard and modified Proctor tests performed on the grain- and powder-mixtures

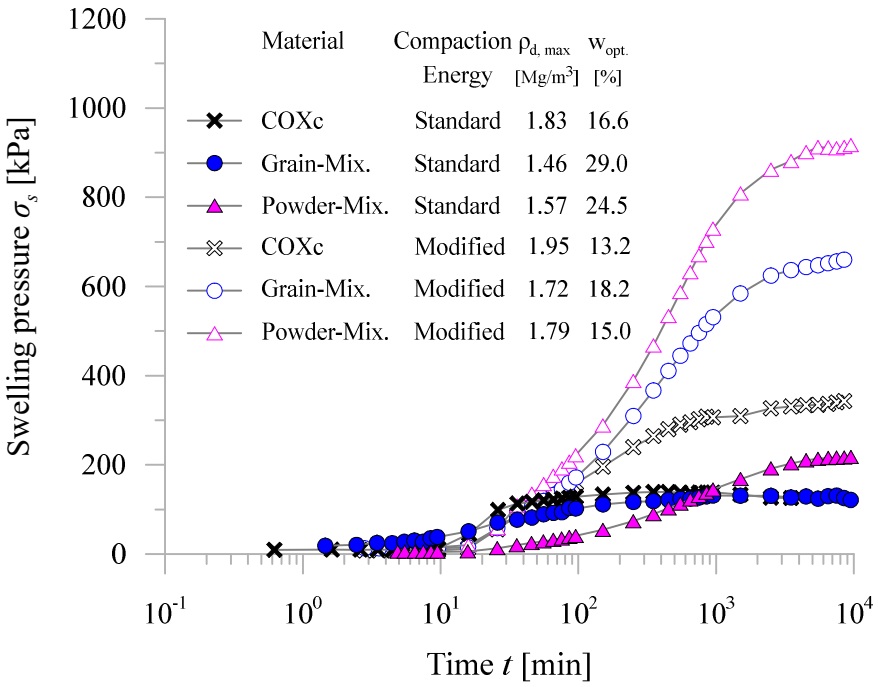


Figure 3: Evolution of swelling pressure of COXc, grain- and powder-mixture compacted to their individual maximum dry densities at optimum water contents and saturated with demineralised/deaired water (DW)

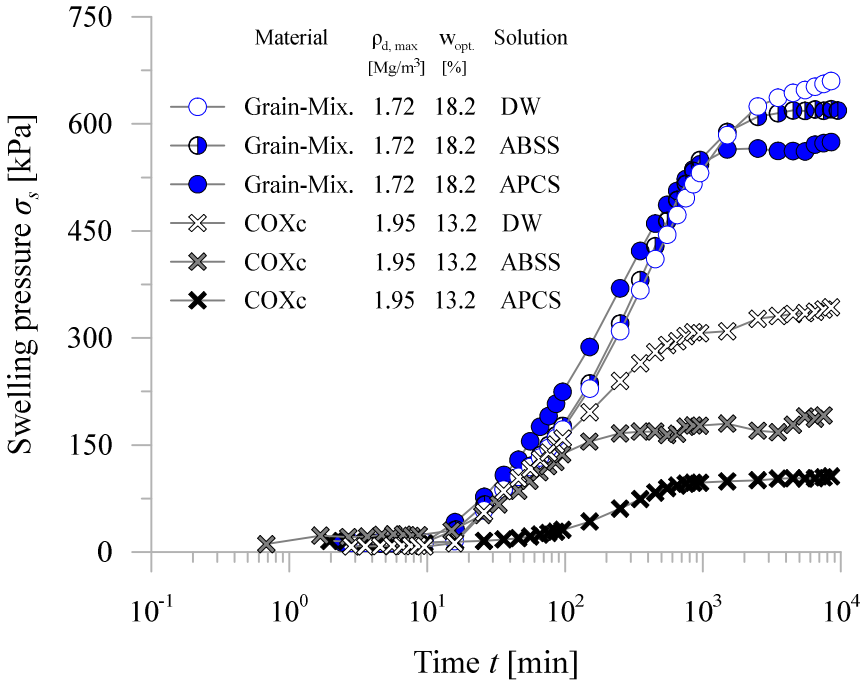


Figure 4: Evolution of swelling pressure of COXc and the grain-mixture compacted to the individual maximum dry densities at optimum water contents and saturated with demineralised/deaired water (DW), artificial Bure site solution (ABSS) and artificial Portland cement solution (APCS))

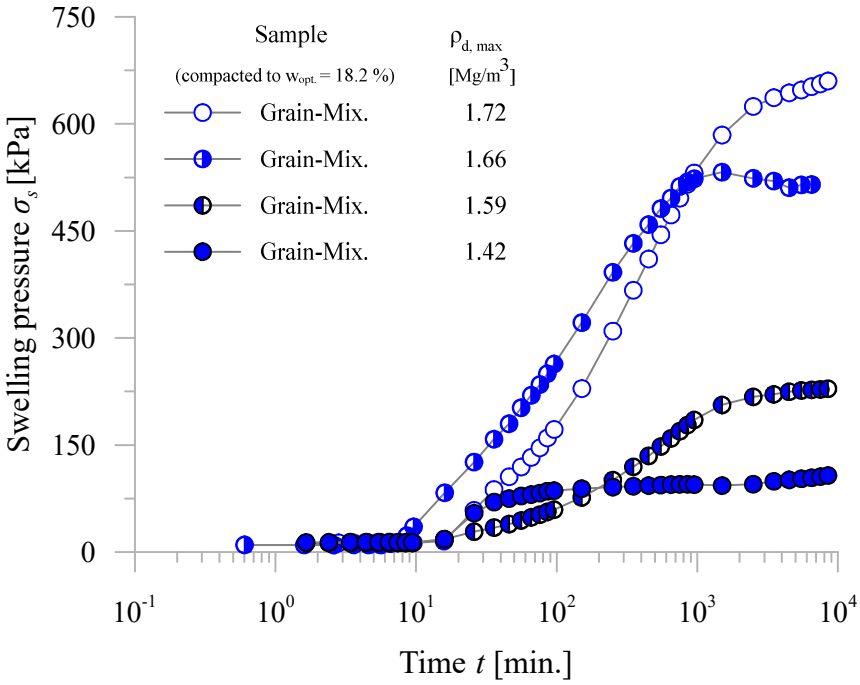


Figure 5: Evolution of swelling pressure of the grain-mixture compacted to 1) maximum dry density, 2) maximum dry density reduced by 3.5%, 3) maximum dry density reduced by 7.5%, and 4) maximum dry density reduced by 17.5% at optimum water content and saturated with deaired/demineralised water (DW)

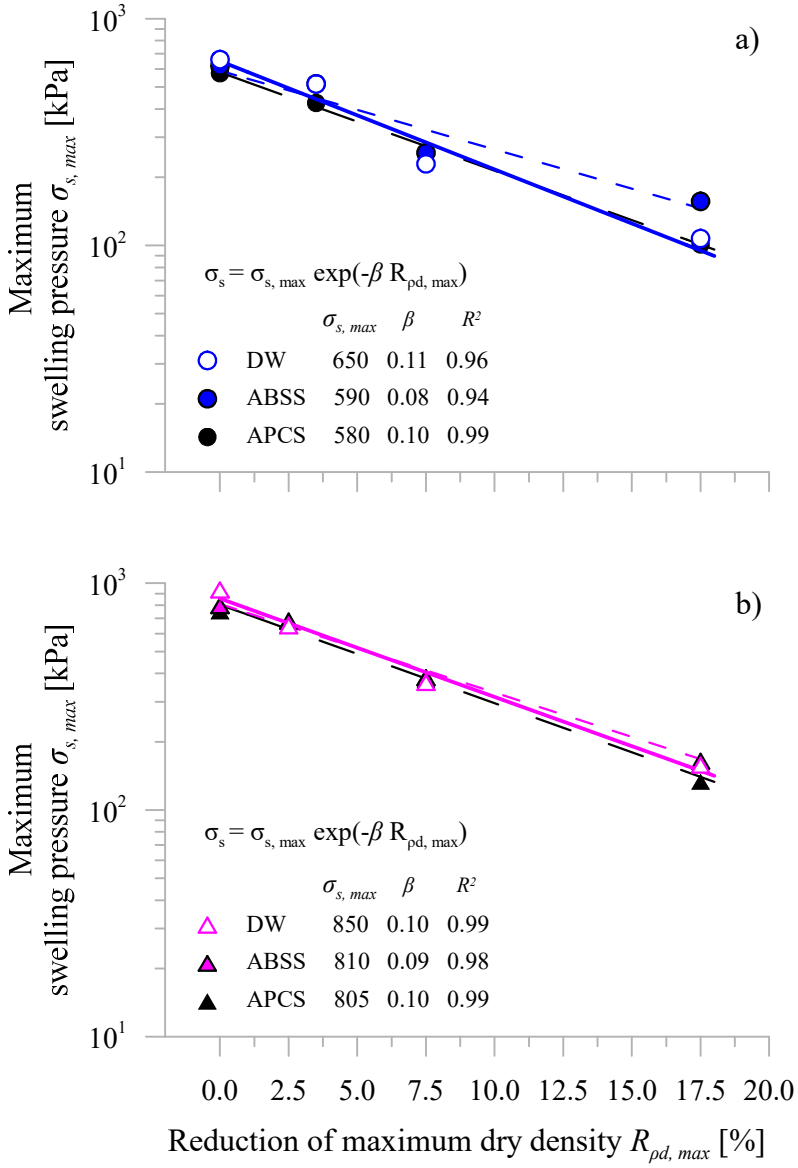


Figure 6: Depiction of the exponential relation between the reduction of initial dry density and the maximum swelling pressure, including the impact of the saturating solution chemistry: a) Relation of grain-mixture, b) Relation of powder-mixture

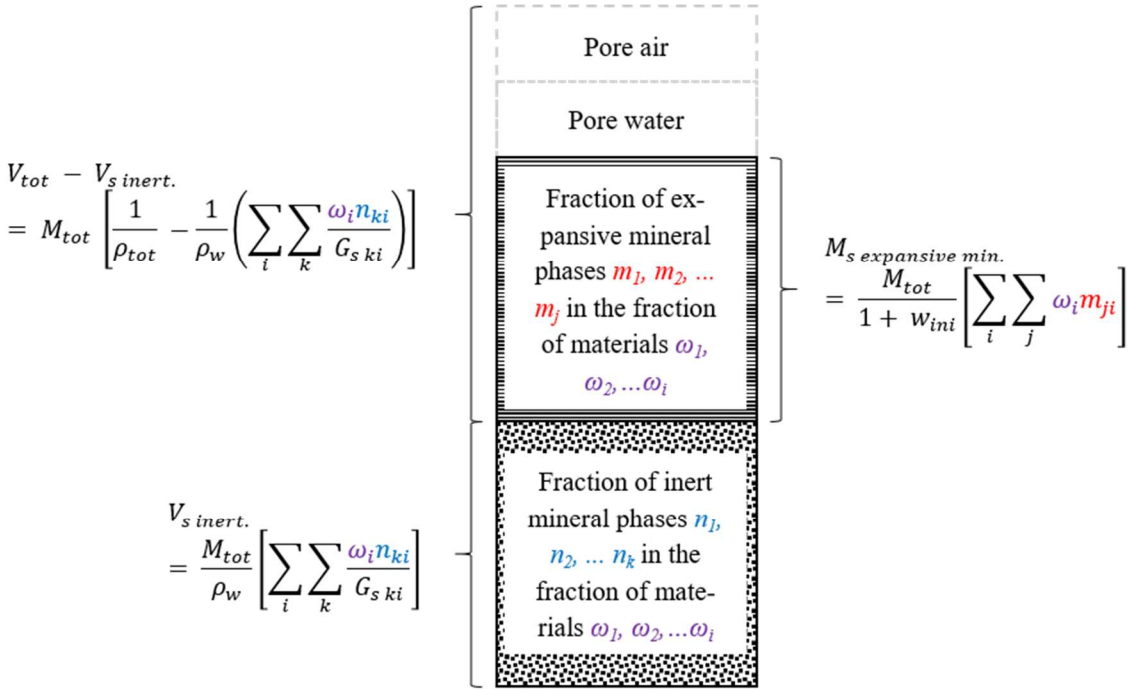


Figure 7: Defined four phases of a mixture composed of different expansive clays

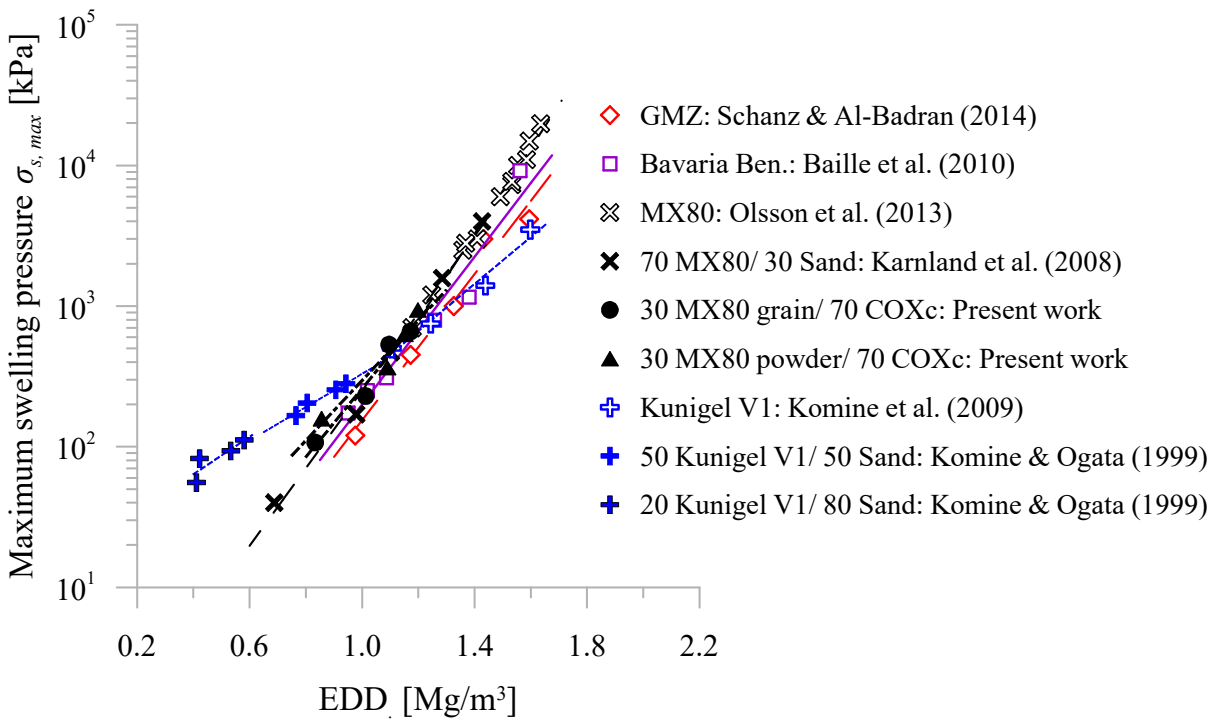


Figure 8: Exponential relationship of EDD and the maximum swelling pressure including results of various expansive clays and their mixtures with varying amounts of non-expansive material taken from the literature

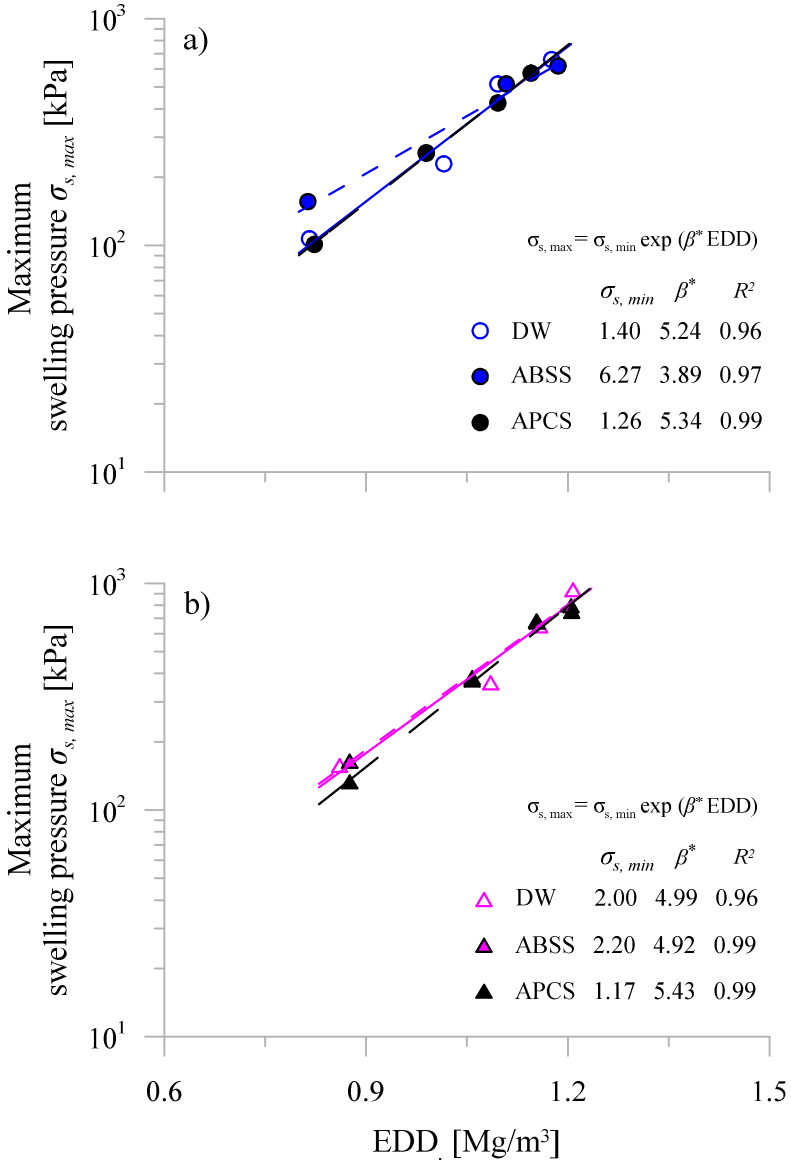


Figure 9: Exponential relation of EDD and maximum swelling pressure in the case of the a) grain-mixture and b) the powder-mixture (saturated with deaired/demineralised water (DW), artificial Bure site solution (ABSS) and artificial Portland cement solution (APCS))

| Mineral | | Müller-Vonmoos and Kahr (1983) | Herbert et al. (2004) | Karnland et al. (2007) |
|---|---|---|---|---|
| Carbonate | [%] | 1 | < 2 | 1 |
| Cristobalite | [%] | - | < 2 | 3 |
| Feldspar | [%] | 7 | 2 | 7 |
| Kaolinite | [%] | < 1 | - | - |
| Mica | [%] | < 1 | - | 1 |
| Montmorillonite | [%] | 75 | 90 | 83 |
| Quartz | [%] | 15 | 4 | 5 |
| Pyrite | [%] | > 1 | > 1 | - |

1 Table 1: Mineralogical composition of MX80-bentonite taken from literature

| **Material** | **Physical properties** | | | | | |
|---|---|---|---|---|---|---|
| | Natural water content | Specific gravity | Liquid limit | Plastic limit | 10 %-Passing | 60 %-Passing |
| | w | $G_s$ | LL | PL | $D_{10}$ | $D_{60}$ |
| | [%] | [-] | [%] | [%] | [mm] | [mm] |
| $COX_c$ | 5.4 | 2.68 | 37.3 | 24.9 | 0.01 | 0.8 |
| MX80[a, b] | - | 2.65 - 2.88 | 420.0 - 520.0 | 38.0 - 65.0 | - | - |
| Grain mix. | 6.4 | 2.64 | 112.5 | 34.7 | 0.008 | 0.8 |
| Powd. mix. | 6.4 | 2.64 | 112.5 | 34.7 | 0.004 | 0.2 |

[a] : Delage et al. (2006)
[b] : Komine et al. (2009)

1 Table 1: Determined physical properties of $COX_c$, MX80-bentonite, grain- and powder-mixture

| | | Artificial Bure Site Solution (ABSS) | Artificial Portland Cement Solution (APCS) |
|---|---|---|---|
| Compound/ Main ion species | | c (Compound) [mmol/l] | c (Compound) [mmol/l] |
| NaCl | | 33.4 | 22.1 |
| $NaHCO_3$ | | 1.5 | - |
| $Na_2SO_4$ | | 4.9 | - |
| KCl | | 0.5 | 8.0 |
| $Ca(OH)_2$ | | - | 19.0 |
| $CaSO_4*2H_2O$ | | 4.6 | - |
| $CaCl_2*2H_2O$ | | 0.7 | - |
| $MgSO_4*7H_2O$ | | 8.5 | - |
| I | [mmol/l] | 105.0 | 87.0 |
| pH | [-] | 7.8 | 12.4 |

c (Compound): Molar concentration of the compound

1 Table 3: Compounds and characteristics of solutions being employed

| **Reference** | **Material** | $\sum\sum f_i x_{ji}$ | $\sigma_{s,\,min}$ | $\beta^*$ | $\mathbf{R^2}$ |
|---|---|---|---|---|---|
| | | [-] | [kPa] | [-] | [-] |
| Schanz and Al-Badran (2014) | GMZ01 bentonite | 0.75 | 0.39 | 5.99 | 0.971 |
| Baille et al. (2010) | Bavaria bentonite | 0.78 | 0.47 | 6.05 | 0.947 |
| Olsson et al. (2013) | MX80 bentonite | 0.83 | 0.15 | 7.59 | 0.907 |
| Karnland et al. (2007) | 70 % MX80/ 30 % Sand | 0.58 | 0.42 | 6.78 | 0.992 |
| Komine et al. (2009) | Kunigel V1 bentonite | 0.57 | 6.60 | 3.85 | 0.975 |
| Komine and Ogata (1999) | 50 % Kunigel/ 50 % Sand | 0.17 | 32.00 | 1.97 | 0.617 |
| Komine and Ogata (1999) | 20 % Kunigel/ 80 % Sand | 0.11 | 18.68 | 2.58 | 0.751 |
| Present work: Grain-mix. | 30 % MX80 gr./ 70 $COX_c$ | 0.35 | 1.40 | 5.24 | 0.962 |
| Present work: Powder-mix. | 30 % MX80 po./ 70 $COX_c$ | 0.35 | 2.00 | 4.99 | 0.963 |

$\sum\sum f_i x_{ji}$ *: Accumulated mass fraction of expansive minerals (in the mixture)*

1 Table 4: Material parameters obtained by correlation of experiment and literature data